

Study of the x-ray emission scaling law in a low energy plasma focus

This article has been downloaded from IOPscience. Please scroll down to see the full text article.

2004 Plasma Sources Sci. Technol. 13 B7

(<http://iopscience.iop.org/0963-0252/13/4/B01>)

View [the table of contents for this issue](#), or go to the [journal homepage](#) for more

Download details:

IP Address: 38.107.179.212

The article was downloaded on 16/02/2012 at 06:10

Please note that [terms and conditions apply](#).

BRIEF COMMUNICATION

Study of the x-ray emission scaling law in a low energy plasma focus

M Sharif¹, S Hussain¹, M Zakaullah¹, and A Waheed²

¹ Department of Physics, Quaid-i-Azam University, 45320 Islamabad, Pakistan

² PINSTECH, PO Box 2151, 44000 Islamabad, Pakistan

E-mail: mzakaullah@qau.edu.pk and zaka_qau_pk@yahoo.com

Received 18 July 2003, in final form 5 March 2004

Published 6 October 2004

Online at stacks.iop.org/PSST/13/B7

doi:10.1088/0963-0252/13/4/B01

Abstract

The performance of a low energy (0.6–1.8 kJ) Mather-type plasma focus (PF) device as a Cu–K α x-ray source is examined. The Cu–K α and total x-ray emissions are measured for argon and hydrogen filling. It is found that Cu–K α emission varies as $Y_K[\text{J}] \sim [E(\text{kJ})]^{3.5-4.5} \sim [I(100\text{ kA})]^{3.5-4.5}$, whereas the total x-ray emission is found to follow $Y_{\text{tot}}[\text{J}] \sim [E(\text{kJ})]^{4.5-5.5} \sim [I(100\text{ kA})]^{4.5-5.5}$. At optimum conditions, the system with discharge energy of 1.8 kJ is found to generate x-rays with $1.44 \pm 0.07\%$ efficiency. About 32% of the emission constitutes the Cu–K α line radiation. With a cut at the anode tip, the x-ray flux in the side-on direction is increased three times. The modified geometry may help in using the PF as a radiation source for x-ray diffraction.

1. Introduction

Soft x-ray sources of high intensity are required in diverse areas like x-ray spectroscopy [1], lithography for the manufacture of integrated circuits [2], x-ray microscopy [3], x-ray laser pumping [4] and x-ray crystallography [5]. Work is underway to develop such sources by employing geometries like Z-pinch [6], X-pinch [7], vacuum spark [8] and plasma focus (PF) [9–11]. The latter is the simplest in construction and yet provides the highest x-ray emission compared to other devices of equivalent energy [12, 13]. Shyam and Sirinivasan [14] reported an experiment to study x-ray emission from a Mather-type PF energized by a 16.8 μF capacitor bank charged at 6–16 kV, providing 100–230 kA peak discharge current. Both hard and soft x-rays were emitted from the device. Liu *et al* [15] studied soft x-ray yield from a PF with a 30 μF single capacitor charged to 14 kV. With neon filling, a total soft x-ray yield of 6 J per shot in 4π steradians was reported which corresponds to 0.2% efficiency, which can be defined as the ratio of the energy emitted as x-rays in 4π -geometry to the energy stored in the capacitor bank. Serban and Lee [16] investigated the soft x-ray emission by employing filtered p-type intrinsic n-type (PIN) diodes. Scaling laws relating the

soft x-ray yield to peak discharge current, peak axial velocity and anode radius were proposed. It was found that the x-ray yield varies as $Y \sim I^n$, where $n = 2-4$. They further reported that for a given operating pressure, the soft x-ray yield increases with the square of the axial speed in the range 7–14 $\text{cm } \mu\text{s}^{-1}$. However, it was described that the proposed scaling law was not so accurate. Castillo *et al* [17] studied the x-ray emission from a PF using a pinhole camera along with a fast PIN diode detector. In addition, a hard x-ray signal was recorded by a photomultiplier tube coupled with a NE-102A plastic scintillator placed outside the chamber. Two x-ray pulses were reported. The maximum of neutron emission appears 50 ns after the first x-ray pulse. The soft x-ray emission during the first pulse was found to be correlated with the neutron emission. Beg *et al* [18] reported the x-ray emission for different filling gases from a 2 kJ PF with peak discharge current of about 200 kA. A maximum x-ray yield of 16.6 J per shot was found with neon filling. The PF was demonstrated as an intense source for x-ray backlighting. Filippov *et al* [19] reported a megajoule PF as an efficient x-ray source. In this work a 9.2 mF capacitor bank was charged up to 14 kV with energy storage of 0.9 MJ at 1 Torr neon. A fast plastic scintillator (0.2 mm thick NE 193) covered with 10 μm Al

was used for x-ray detection. Ten per cent of the capacitor bank energy was reported to convert into K-shell lines of Ne radiation. A scaling law $Y_x \sim I_p^{3.5-4}$ was proposed, where Y_x and I_p are the x-ray yield and the pinch current, respectively. It was reported that the x-radiation of Ne-plasma is many times more intense than that measured during operation in pure deuterium. The Ne-plasma sheath attains velocity of $(2-3) \times 10^7 \text{ cm s}^{-1}$ in the final compression phase. Zakaullah *et al* [20] investigated x-radiation emission with argon filling in a 2.3 kJ PF. The emitted radiation in the Al(1.2–1.56 keV) and Ti(2.9–4.96 keV) windows were found suitable for backlighting. Shafiq *et al* [21] studied x-ray emission with nitrogen filling in the 1.2–1.3 keV and 1.2–1.5 keV windows with discharge energy of 1.15 kJ. The total emission in 4π -geometry in the corresponding intervals was 1.03 J per shot and 14 J per shot, respectively. The corresponding efficiencies were found to be 0.04 and 1.22%. The total energy emitted as x-rays was estimated 21.8 J per shot with corresponding efficiency of 1.9%. Zakaullah *et al* [22] investigated x-ray emission in 2.3 kJ PF system with neon filling. At optimum conditions, the x-ray yield for cylindrical anode was 7 J per shot, which increased to 80 J per shot for tapered anode. The latter corresponds to an efficiency of 4%.

In this paper, Cu– K_α and soft x-rays ($\leq 10 \text{ keV}$) emission from a low energy PF operated with argon and hydrogen filling and energized with a $9 \mu\text{F}$ capacitor bank charged at 12–20 kV is studied. Attention is paid to establish x-ray yield scaling law with discharge energy and peak discharge current. Further, the experiment is conducted by shaping the anode tip at various angles with reference to the focus axis for tailoring higher x-ray flux in the side-on direction. Section 2 discusses the spectral technique for x-ray analysis, whereas section 3 presents the experimental setup and diagnostics. In section 4, results and discussions are given, and conclusions are described in section 5.

2. Spectral analysis of x-rays

The dispersive techniques for spectral analysis of x-rays require the use of delicate equipment, which is not available in this laboratory. Therefore, a combination of Ross filters [23] and fast PIN diodes is used for spectral analysis. When x-rays pass through a foil of a material, the following effects are taken into consideration:

- (i) High energy photons observe less absorption, whereas low energy photons experience high absorption.
- (ii) Transmission of photons experiences a sudden jump for the energies, which are equal to the ionization energies of the material from K, L, M, etc, energy levels.

A pair of filters, known in the literature as Ross filters [23], can be selected for the desired energy window. By reviewing the transmission windows of different commercially available filters, the selected Ross filter pair is Ni (17.5 μm) and Co (20 μm). The transmission curves for these filters are presented in figure 1(a). We have used Quantrad Si PIN diodes of active layer thickness 125 μm . The detectors' response along with transmission characteristics of the filters is given in figure 1(b). For the evaluation of these curves, the data for absorption coefficients were taken from the Handbook of

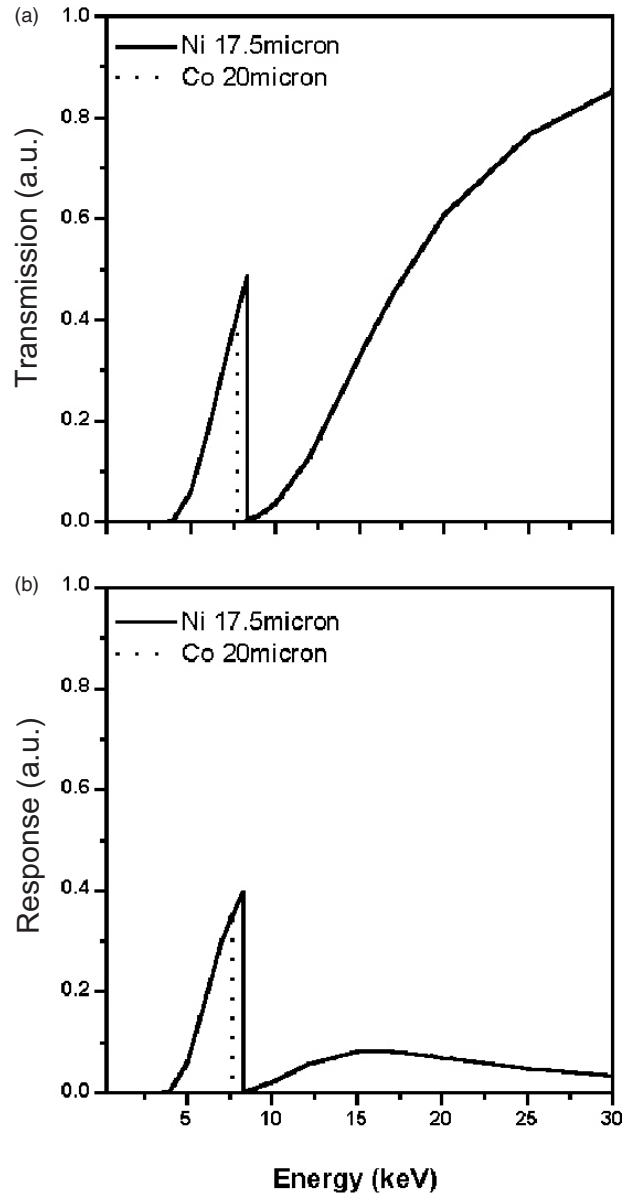


Figure 1. (a) Transmission curves of Ni (17.5 μm) and Co (20 μm) filters and (b) response of PIN diode detectors along with respective filters.

Spectroscopy [24]. The Co filter has the absorption edge at 7.70 keV, and allows transmission of x-rays in the 4–7.70 keV window. The absorption edge of Ni lies at 8.33 keV and allows transmission of Cu– K_α line of 8.05 keV. Thus, the difference of transmission for the Ni and Co filters corresponds to Cu– K_α line radiation.

3. Experimental set-up and diagnostics

The schematic of Mather-type PF system employed in this experiment is shown in figure 2. It is energized by a $9 \mu\text{F}$ capacitor bank whose detail is given elsewhere [25], charging it at different voltages in the range 12–20 kV (0.6–1.8 kJ) and giving peak discharge current of about 100–175 kA. A triggertron-type pressurized sparkgap [26] is used as a switch for transfer of the stored energy in the capacitor bank to the

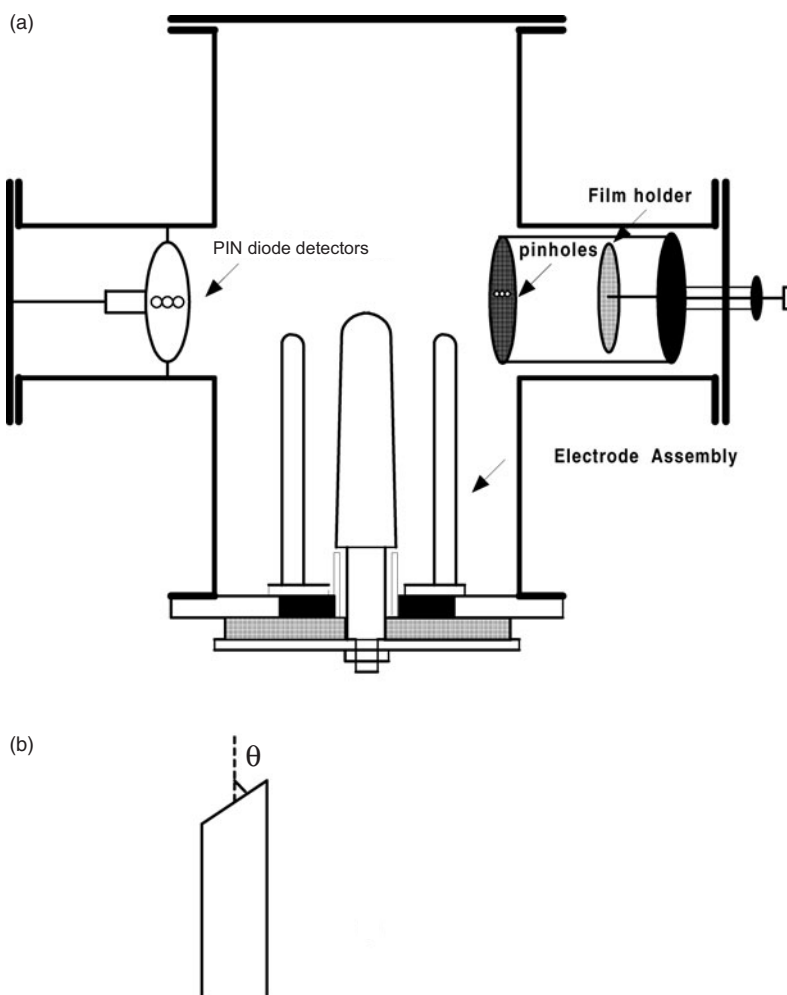


Figure 2. (a) A schematic of the PF electrodes and diagnostics. (b) The anode tip with a cut.

system. The electrode system comprises a copper rod of 96 mm in length and 20 mm in diameter as an anode, which is slightly tapered towards the open end [27]. Another experiment is performed for two other cylindrical anodes with a cut at $\theta = 45^\circ$ and 76° with anode axis as shown in figure 2. Six copper rods each of 9 mm diameter surround it such that the ratio of cathode to anode radii is 3.2. The PF chamber is evacuated up to 10^{-2} mbar using a rotary vane pump. The experiment is conducted with argon and hydrogen as filling gases and eight shots are recorded for each filling pressure. After recording four shots, the old gas is purged and fresh gas is filled to minimize the effects of impurities. For monitoring the x-ray emission in different shots, the Quantrad Si PIN diodes of $125 \mu\text{m}$ active layer thickness along with suitable absorption filters are used. These detectors were placed in the side on direction at 14.5 ± 0.2 cm from the anode axis, and elevated at 1.5 ± 0.1 cm from the anode tip. For the safety of each diode a 0.6 mm thick brass disc with 2 mm-diameter hole at the centre was used. The intensity of x-rays from the focus region is found measurable for argon and hydrogen within the pressure ranges of 0.25–2.5 mbar and 0.25–5.0 mbar, respectively; below and above these pressure ranges it attains very small values. For time-integrated x-ray measurement, a pinhole camera with three pinholes each of $200 \mu\text{m}$ in diameter is employed. The

electrical signals from the two PIN diodes, high voltage (HV) probe and Rogowski coil were recorded by a four channel 200 MHz Gould 4074A digital storage oscilloscope and the data were transferred to a computer through a general purpose interface bus (GPIB) 488.2.

4. Results and discussion

Figure 3(a) depicts the variation of Cu- K_α yield and corresponding efficiency at an optimum pressure of 1.0 mbar argon filling versus discharge current, charging voltage and stored energy. It indicates that Cu- K_α yield varies approximately following a scaling law:

$$Y_K[\text{J}] \sim [E(\text{kJ})]^{3.5-4.5} \sim [I(100 \text{ kA})]^{3.5-4.5},$$

where $Y_K[\text{J}]$ is the yield of Cu- K_α radiation (in joules), E is the discharge energy of the capacitor bank (in kilojoules), and I is the peak discharge current (in 100 kA). The technique for estimating the x-ray yield from a point source is reported elsewhere [28, 29]. A maximum Cu- K_α yield of about 8.30 ± 0.42 J per shot in 4π -geometry is recorded for 175 ± 5 kA discharge current and the corresponding efficiency is about $0.46 \pm 0.02\%$. Figure 3(a) also shows that Cu- K_α yield rapidly

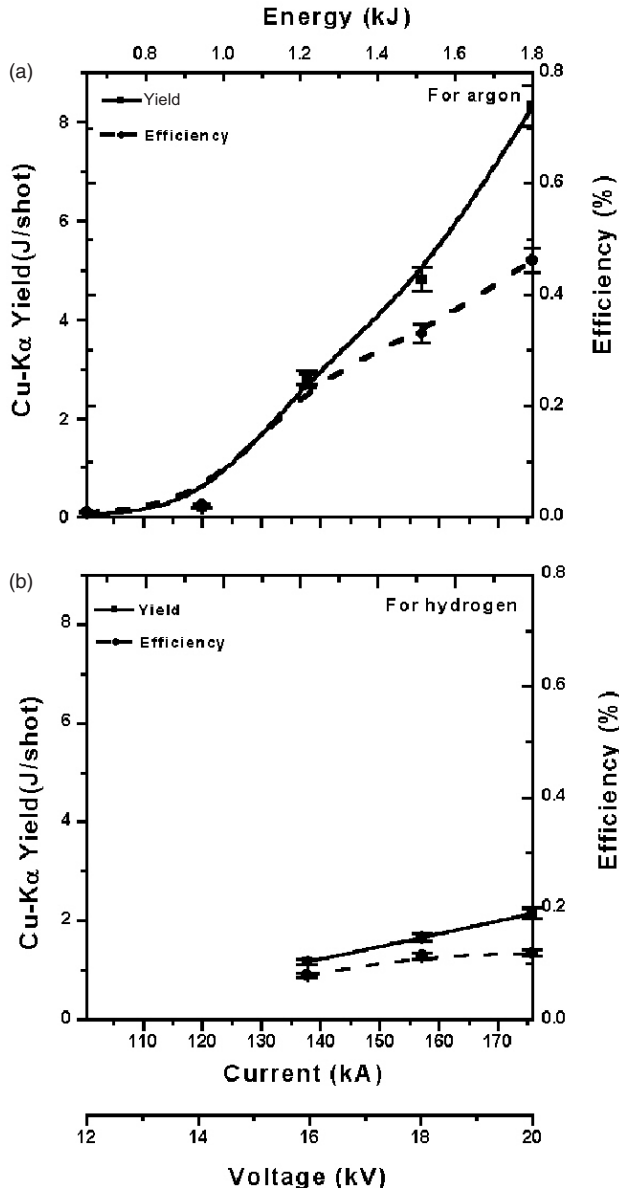


Figure 3. The variation of Cu-K α yield and efficiency versus discharge current, charging voltage and discharge energy for: (a) argon, (b) hydrogen gas filling.

increases for charging voltage exceeding 16 kV, and it is low for lower voltages.

Figure 3(b) is a representation of the variation of Cu-K α yield and the corresponding efficiency for current, voltage and energy at an optimum pressure of 3.0 mbar for hydrogen. A comparison of the graphs given in figure 3 shows the following results:

- (i) The Cu-K α yield is small for charging voltage less than 16 kV.
- (ii) The optimum pressure for argon and hydrogen is different.
- (iii) The Cu-K α yield and efficiency for argon is about four times higher than that of hydrogen.
- (iv) Slopes of graphs for argon are relatively higher than that of hydrogen, which show more variation in Cu-K α yield compared to that of hydrogen.

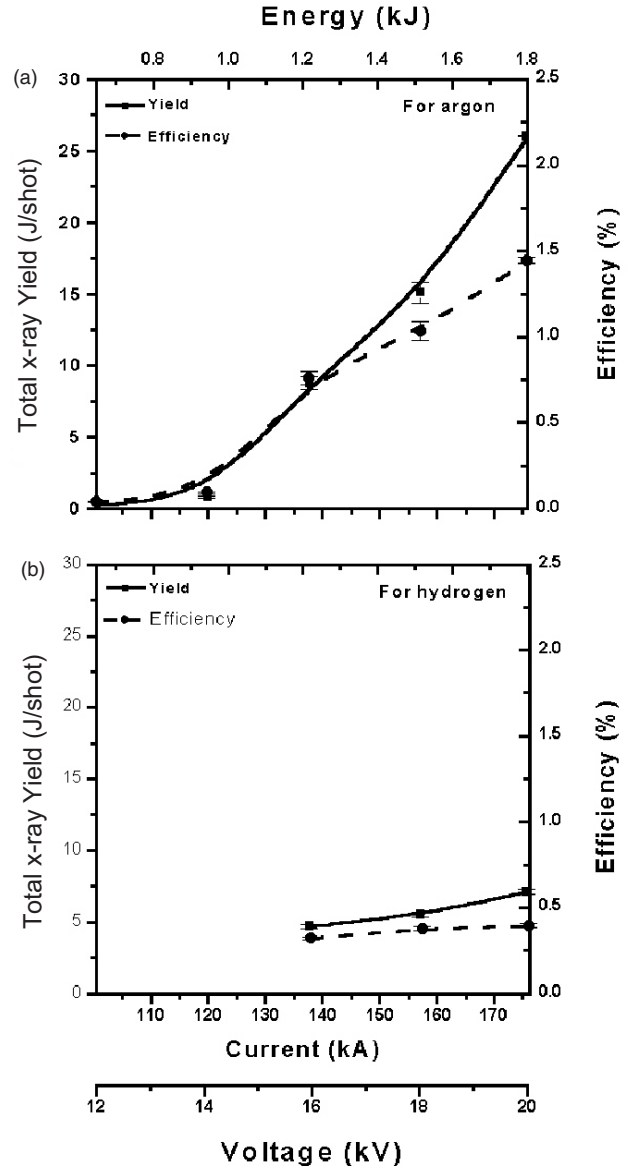


Figure 4. The variation of total x-ray yield and wall-plug efficiency versus discharge current, charging voltage and discharge energy for: (a) argon, (b) hydrogen gas filling.

Figure 4(a) demonstrates the variation of total x-ray yield and corresponding efficiency at an optimum pressure of 1.0 mbar argon versus current, charging voltage and capacitor bank energy. It shows that the yield varies approximately following a scaling law:

$$Y_{\text{tot}}[\text{J}] \sim [E(\text{kJ})]^{4.5-5.5} \sim [I(100 \text{ kA})]^{4.5-5.5},$$

where $Y_{\text{tot}}[\text{J}]$ is the total x-ray yield (in joules), E is the discharge energy of the capacitor bank (in kilojoules) and I is the peak discharge current (in 100 kA). In 4π -geometry a maximum soft x-ray yield of about $26.02 \pm 1.30 \text{ J}$ per shot is recorded for $175 \pm 5 \text{ kA}$ current and the corresponding efficiency is about $1.44 \pm 0.07\%$. It is evident from the graphs that the x-ray yield increases rapidly with the increase in discharge energy and current. However, to check the saturation, if any, one needs bigger systems operating at higher

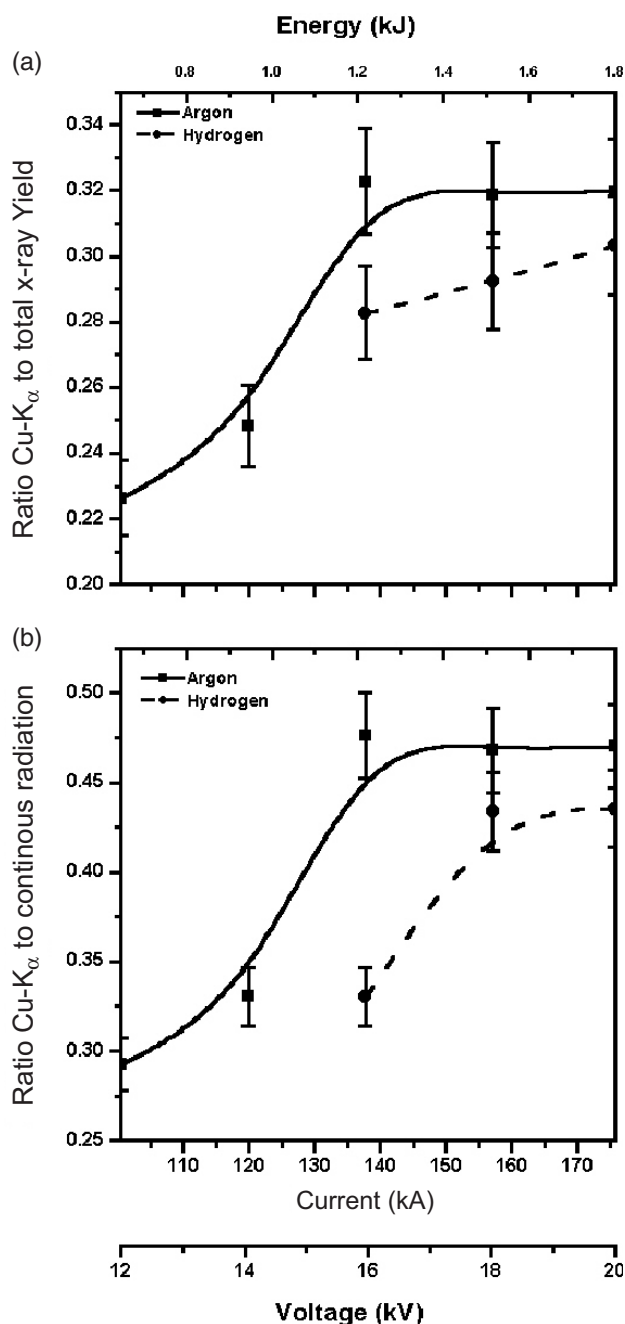


Figure 5. The variation of the ratio of Cu-K α to: (a) total x-ray yield, (b) continuous radiation versus discharge current, stored energy and charging voltage at optimum pressures of argon and hydrogen gas pressure.

voltages. Figure 4(b) represents the same at 3.0 mbar, the optimum pressure of hydrogen for the highest emission.

Figure 5(a) shows how the ratio of Cu-K α and total x-ray yield varies with variation of the discharge current, stored energy and charging voltage at optimum pressures of argon and hydrogen. It increases with increasing discharge current up to 135 ± 5 kA beyond which it saturates. The highest ratio recorded is 0.32 ± 0.02 , for argon gas filling. In this system, this discharge current corresponds to 1.15 kJ stored energy in the capacitor bank. It is speculated that the increase in charging voltage leads to deep penetration of energetic electrons in the meat of the anode, resulting in enhanced self-absorption

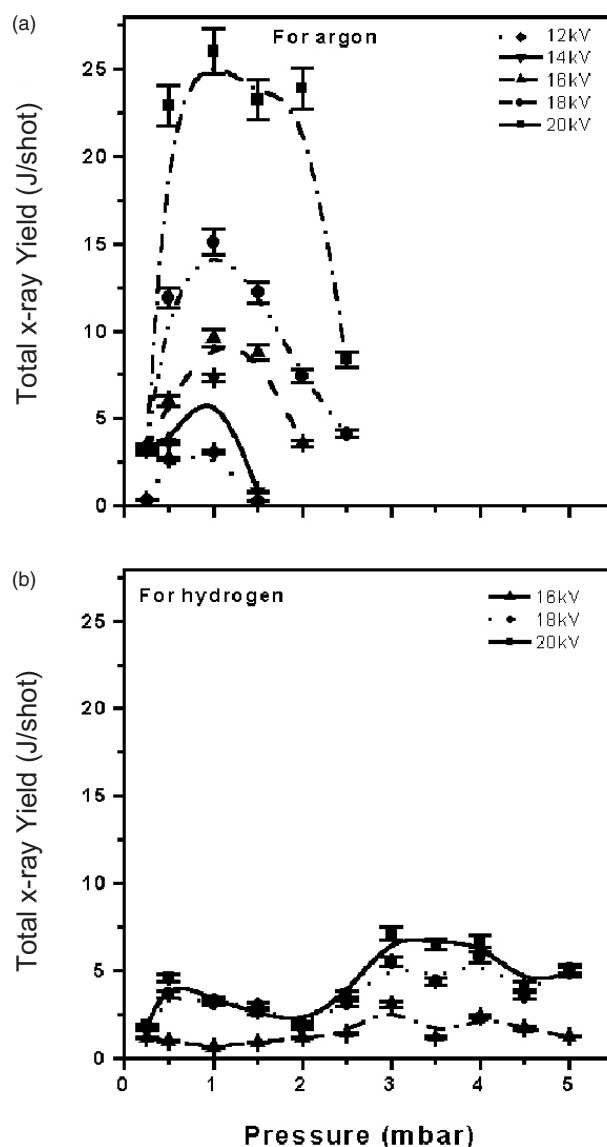


Figure 6. The variation of total x-ray yield at different charging voltages versus pressure for: (a) argon, (b) hydrogen gas filling.

and lower recording by the detector. Figure 5(b) depicts the variation of the ratio of Cu-K α to continuous radiation yield with discharge current, stored energy and charging voltage at optimum pressures of argon and hydrogen. This ratio attains a peak value at 16 kV for argon and 18 kV for hydrogen. Figure 6 summarizes the variation of total x-ray yield versus argon and hydrogen pressures for different charging voltages.

In a conventional x-ray tube, the ratio of characteristic Cu-K α to continuous radiation varies with the applied voltage. It increases up to 40 kV, and attains a value of 0.75 [30]. With the increase in potential difference, this ratio decreases again. However, the comparison of the results of a conventional x-ray tube with the PF may not be a straightforward task. In an x-ray tube, the electrons may be considered monoenergetic and the energy is well defined. In a PF, the electrons' energy striking the anode tip may have a wide spectrum [31]. It will be interesting to estimate the characteristic radiation emission at different charging voltages and the electron beam energy

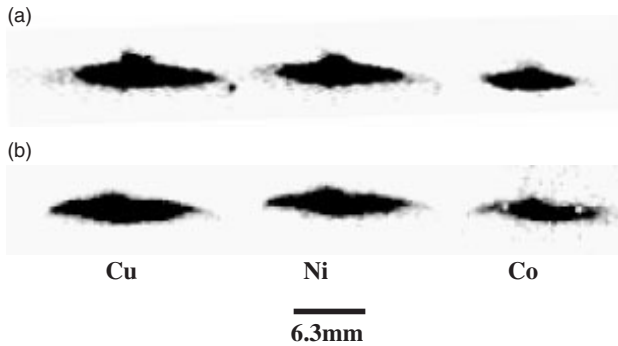


Figure 7. X-ray pinhole ($200\ \mu\text{m}$ each) images masked with Cu ($10\ \mu\text{m}$), Ni ($12.5\ \mu\text{m}$) and Co ($10\ \mu\text{m}$) filters: (a) argon at 1.0 mbar, (b) hydrogen at 3.0 mbar.

spectrum in PF devices. The work is in progress and will be reported later.

Serban and Lee [16], have proposed scaling law for total x-ray emission from a 3 kJ PF device, which states $Y_{\text{sx}} \sim I^n$ and/or $Y_{\text{sx}} \sim I^n v_{\text{axial}}^n$ with $n = 2-4$. Filippov *et al* [19] reported that x-ray emission varies $Y_x \sim I_p^{3.5-4}$, in a large PF facility operated at 0.9 MJ discharge energy. The results of these experiments are in agreement with the scaling law proposed in this work, which is more comprehensive and detailed.

Photographs of the plasma region obtained by a pinhole camera [32] mounted in the side-on direction are shown in figure 7. The x-rays from the focus region and anode tip after passing through the three pinholes covered with Cu ($10\ \mu\text{m}$), Ni ($12.5\ \mu\text{m}$) and Co ($10\ \mu\text{m}$) filters fall on the photographic film which is fixed in a holder. The soft x-rays emitted from the plasma column are not transmitted by the filters and this region is not visible. The images with Co filter are fainter than those obtained with Cu and Ni filters which is in agreement with the data recorded by the PIN diodes. This is representative of the fact that a significant amount of x-rays emitted from the anode tip is Cu- K_α , for which the Co filter is opaque.

Development of an x-ray diffractometer using PF as the radiation source and x-ray film as the detector, in the Debye-Scherrer camera arrangement is planned. Due to high ion beam flux in the end-on direction, the emitted x-rays may not be used to this end. For obtaining higher x-ray flux in the side-on direction, the anode end was cut at angles of 45° and 76° , as shown in figure 2(b). In this experiment, the anode is of cylindrical shape, that is, it is without any tapering. Data analysis shows that the x-ray flux in the side-on direction is higher for 76° as compared to that of 45° cut. It is found that the x-ray flux in the side-on direction for a cut at 76° is approximately two and half times higher compared to the case of a tapered anode. It is estimated that the observed flux corresponds to 1.3×10^{15} Cu- K_α photons sr^{-1} per shot, when the PF is operated at 20 kV charging voltage. The PF operation with the anode having an angled cut at the tip helped in obtaining high x-ray flux accompanied by insignificant charge particle flux (contrary to the end-on direction). Further, the damage at the anode face by impact of the energetic electron beam is not at the centre. It is speculated that due to the cut, current sheath travels unequal distances in the radial direction in the compression phase. As a result the plasma is not

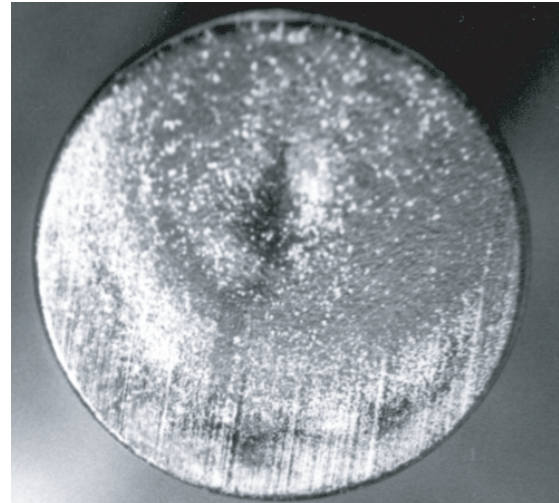


Figure 8. Photograph of the face of the cut anode after about 50 shots at 18 kV charging voltage.

compressed at the anode axis and the electron beam generated from the PF region does not hit the axial point of the anode. Figure 8 presents the photograph of the anode tip after about 50 shots. Further work is underway and will be reported later.

5. Conclusions

In conclusion, x-ray emission from a low energy (0.6–1.8 kJ) Mather-type PF operated at different voltages, and with argon and hydrogen as the filling gases is studied by employing time-resolved and time-integrated detectors. For 20 kV charging voltage, the highest x-ray yield is recorded at filling pressures of 1 mbar and 3 mbar of argon and hydrogen, respectively. The Cu- K_α and total x-ray emission in 4π -geometry at optimum pressure of argon is about 8.30 ± 0.42 J per shot and 26.02 ± 1.30 J per shot, respectively. For 3 mbar of hydrogen filling, the highest total soft x-ray emission in 4π -geometry is about 7.10 ± 0.36 J per shot, about 2.2 ± 0.11 J per shot of which is the Cu- K_α emission. A scaling law is proposed which relates x-ray emission to discharge energy and discharge current.

Acknowledgments

This work was partially supported by Quaid-i-Azam University Research Grant, Ministry of Science & Technology, Pakistan Science Foundation Project No PSF/R&D/C-QU/Phys (199), Higher Education Commission Project for Plasma Physics, Pakistan Atomic Energy Commission Project for Plasma Physics, the Abdus Salam International Center for Theoretical Physics, Trieste, Italy Project AC-7 Islamabad and ICSC—World Laboratory Project E-13 CHEPCI Islamabad.

References

- [1] Pearlman J S and Roirdan J C 1981 *J. Vac. Sci. Technol.* **19** 1190
- [2] Feder R, Pearlman J S, Riordan J C and Costa L J 1984 *J. Microsc.* **135** 347
- [3] Niemann B, Rudolph D, Schmahl G, Diehl M, Thieme J, Neff W, Holz R, Lebert R, Richter F and Herziger G 1989 *Optik* **84** 35

- [4] Porter J L, Spielman R B, Matzen M K, Macguire E J, Ruggles L E and Vargas M F 1992 *Phys. Rev. Lett.* **68** 796
- [5] Rocca J J, Shlyaptsev V, Tomasel F G, Cortazar O D, Hartshorn D and Chilla J L A 1994 *Phys. Rev. Lett.* **73** 2192
- [6] Kantsyrev V L, Kopytok K I and Shlyaptseva A S 1993 *Proc. 3rd Int. Conf. on Dense Z-pinches (London, UK)* vol 299, ed M Haines and A Knight (New York: AIP) p 226
- [7] Hammer D A, Kalantar D H, Mittal K C and Qi N 1990 *Appl. Phys. Lett.* **57** 2083
- [8] Ikhlef A and Skowronek M 1993 *Proc. 3rd Int. Conf. on Dense Z-pinches (London, UK)* vol 299, ed M Haines and A Knight (New York: AIP) p 218
- [9] Wong C S and Lee S 1984 *Rev. Sci. Instrum.* **55** 1125
- [10] Mather J W 1965 *Phys. Fluids* **8** 366
- [11] Zakaullah M, Akhtar I, Murtaza G and Waheed A 1999 *Phys. Plasmas* **6** 3188
- [12] Zakaullah M, Alamgir K, Shafiq M, Hassan S M, Sharif M and Waheed A 2001 *Appl. Phys. Lett.* **78** 877
- [13] Lee S, Lee P, Zhang G, Feng X, Gribkov V A, Liu M, Serban A and Wong T K S 1998 *IEEE Trans. Plasma Sci.* **26** 1119
- [14] Shyam A and Srinivasan M 1983 *Paramana* **20** 125
- [15] Liu M, Feng X, Stuart V S and Lee S 1998 *IEEE Trans. Plasma Sci.* **26** 135
- [16] Serban A and Lee S 1997 *Plasma Sources Sci. Technol.* **6** 78
- [17] Castillo F, Milanese M, Moroso R and Pouzo J 2000 *J. Phys. D: Appl. Phys.* **33** 141
- [18] Beg F N, Ross I, Lorenz A, Worley J F, Dangor A E and Haines M G 2000 *J. Appl. Phys.* **88** 3225
- [19] Filippov N V, Filippova T I, Khutoretskaia I V, Mialton V V and Vinogradov V P 1996 *Phys. Lett. A* **211** 168
- [20] Zakaullah M, Alamgir K, Shafiq M, Sharif M and Waheed A 2002 *IEEE Trans. Plasma Sci.* **30** 2089
- [21] Shafiq M, Hussain S, Sharif M and Zakaullah M 2001 *J. Fusion Energy* **20** 113
- [22] Zakaullah M, Alamgir K, Shafiq M, Hassan S M, Sharif M, Hussain S and Waheed A 2002 *Plasma Sources Sci. Technol.* **11** 377
- [23] Johnson D J 1974 *Rev. Sci. Instrum.* **45** 191
- [24] Robinson J W 1974 *Hand Book of Spectroscopy* vol 1 (Cleveland, OH: CRC Press) pp 59–61
- [25] Shafiq M, Sartaj, Hussain S, Sharif M, Ahmad S, Zakaullah M, Waheed A, Murtaza G and Ahmad R 2002 *Mod. Phys. Lett. B* **16** 309
- [26] Zakaullah M, Samia Kausar, Imtiaz Ahmad, Murtaza G and Beg M M 1993 *Mod. Phys. Lett. B* **7** 835
- [27] Zakaullah M, Imtiaz Ahmad, Omar A, Murtaza G and Beg M M 1996 *Plasma Sources Sci. Technol.* **5** 544
- [28] Zakaullah M, Alamgir K, Murtaza G and Waheed A 2000 *Plasma Sources Sci. Technol.* **9** 592
- [29] Zakaullah M, Alamgir K, Shafiq M, Sharif M, Waheed A and Murtaza G 2000 *J. Fusion Energy* **19** 143
- [30] Dyson N A 1990 *X-rays in Atomic and Nuclear Physics* (Cambridge: Cambridge University Press) p 120
- [31] Bostick W H, Kilic H, Nardi V and Powel C W 1993 *Nucl. Fusion* **33** 413
- [32] Zakaullah M, Akhtar I, Waheed A, Alamgir K, Shah A Z and Murtaza G 1998 *Plasma Source Sci. Technol.* **7** 206